Chemical Science

Accepted Manuscript

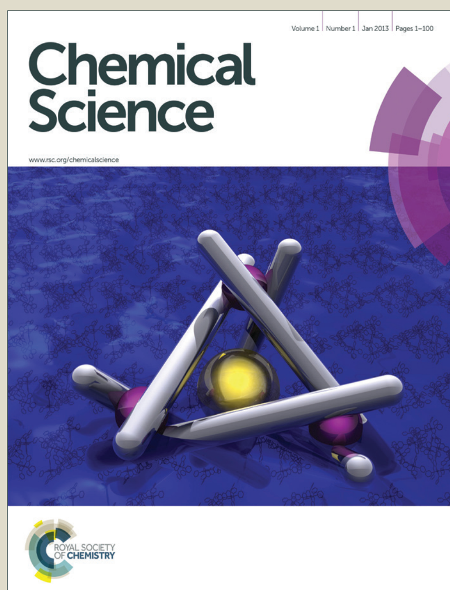

This is an *Accepted Manuscript*, which has been through the Royal Society of Chemistry peer review process and has been accepted for publication.

Accepted Manuscripts are published online shortly after acceptance, before technical editing, formatting and proof reading. Using this free service, authors can make their results available to the community, in citable form, before we publish the edited article. We will replace this *Accepted Manuscript* with the edited and formatted *Advance Article* as soon as it is available.

You can find more information about *Accepted Manuscripts* in the Information for Authors.

Please note that technical editing may introduce minor changes to the text and/or graphics, which may alter content. The journal's standard Terms & Conditions and the Ethical guidelines still apply. In no event shall the Royal Society of Chemistry be held responsible for any errors or omissions in this *Accepted Manuscript* or any consequences arising from the use of any information it contains.

ROYAL SOCIETY OF CHEMISTRY

www.rsc.org/chemicalscience

Chemical Science Accepted Manuscript

Invited Perspective

Synthesis of two-dimensional materials via chemical vapor deposition

Jingxue Yu,[a] Jie Li,[a] Wenfeng Zhang[a] and Haixin Chang[a,*]

[a] Center for Joining and Electronic Packaging, State Key Laboratory of Material Processing and Die & Mould Technology, School of Materials Science and Engineering, Huazhong University of Science and Technology, Wuhan 430074, China.

E-mail: hxchang@hust.edu.cn

Abstract

Two-dimensional (2D) materials have attracted many attentions due to the unique properties and great potentials in various applications. Controllable synthesis of 2D materials with high quality and high productivity is essential for their large scale applications. Chemical vapor deposition (CVD) has been one of the most important and reliable techniques for the synthesis of 2D materials. In this Perspective, the recent advance on CVD growth of three typical types of two-dimensional materials such as graphene, boron nitride and transitional metal dichalcogenides (TMDs) is briefly introduced. Large area preparation, single crystal growth and some mechanism insight are discussed with details. Finally we give a brief comment on the challenges of CVD growth of 2D materials.

Introduction

Chemical vapor deposition (CVD) is a time-honored technique that dates back to centuries ago. The first industrial application of the CVD technique could be traced back to 1897 when de Lodyguine [1]reduced tungsten hexachloride by hydrogen to deposit tungsten onto carbon filament of lamps. CVD was then developed as a reliable extraction method to produce highly purified materials such as Ti, Ta, Zrand Si. For example, Siemens method and its modifications[2] are currently applied in mass production of high-purity polycrystalline silicon, which is vital for the final production of single crystal silicon. Despite the massive application of CVD, it is only in the past half century that the in-depth insight of the process has been made[3]. Now CVD has already been recognized as a reliable synthetic method for zero-dimensional nanomaterials (quantum dots and nanocrystals) and one-dimensional nanomaterials (nanowires and nanotubes, etc.).

Two-dimensional (2D) materials have attracted many attentions due to the unique properties and great potentials in various applications. Controllable synthesis of two-dimensional materials with high quality and high productivity is essential for

Chemical Science Accepted Manuscript

their large scale applications. The methods for synthesis of two-dimensional materials mainly include mechanical exfoliation, liquid phase routes, and CVD. Mechanical exfoliation of bulk materials is able to acquire final product of highest quality with very limited productivity. Liquid phase reactions, such as chemical exfoliation and hydrothermal or solvothermal reactions, have high productivity but the size of sheets is usually small and the quality of the product is relatively low and difficult to control compared with mechanical exfoliations. CVD, on the other hand, offers a compromise between quality, productivity, consistency, and control over the process. The productivity is much higher than mechanical exfoliation, and the quality control is better than liquid phase routes. Therefore CVD has been recognized as a reliable route for preparing high quality two-dimensional (2D) materials recently.

Typically, CVD growth of 2D materials involves activated chemical reactions of precursors in a specially-designed environment. The precursors, conditions, atmospheres, substrates and catalysts (if necessary) are several key factors affecting the final quality of 2D materials. Much progress has been made in preparing 2D materials by CVD and many challenges are needed to be addressed. Herein, we briefly review CVD growth of several signature layered two-dimensional materials such as graphene, BN, and transitional metal dichalcogenides (TMDs), focusing mainly on precursors, conditions, substrates and the end products. The advance in the preparation of large area and single crystal two-dimensional materials are introduced briefly with some discussion of mechanism, and only a small part of the excellent workis included due to the limited space.

CVD growth of Graphene

Ever since the first discovery in 2004 and receiving the Nobel Prize in physics in 2010[4], graphene has been a point of interest for the scientific community. The first graphene sample is prepared via exfoliation by Scotch tapes, which exhibits limited productivity despite the top quality of all the available methods. Other methods are developed to synthesize graphene in order to improve the productivity, such as

Chemical Science Accepted Manuscript

liquid-phase exfoliation, reduction of graphene oxides and bottom-up methods including chemical vapor deposition. Due to the single-atomic-thick nature of graphene film, the growth of graphene via CVD needs a delicate control of the CVD process.

As suggested by theoretical modeling analysis and indicated by the experimental results, the mechanism of catalyzed CVD growth of graphene is similar to the early stage of catalyzed CVD growth of carbon nanotubes[5, 6]. The catalyst, however, is in a shape of films for graphene rather than grains or droplets for carbon nanotubes. With additional manipulation of the reaction parameters, graphene synthesis is favored over carbon nanotubes. Transitional metals (Cu and Ni)[7, 8], rare-earth metals (Ru)[9], noble metals (Pt) [10]and other metals or even compounds have been reported as catalyst for CVD growth of graphene. Transitional metals are believed to be the most efficient catalysts, especially after pre-reaction modification or with certain crystal orientation, and are relatively cheap compared with noble and rare-earth metals [11].Transitional metals can work as both synthesizing substrates and catalysts, and are easily removed to obtain free-standing graphene without compromising the integrity of the grown graphene. It should be noted that the CVD growth mechanisms of graphene with Cu and Ni as catalysts are different. Carbon isotope labeling confirmed that CVD growth of graphene with Cu catalyst is a surface adsorption process, while CVD growth of graphene with Ni catalyst is a diffusion followed by segregation and precipitation process of C on Ni surface[12] .

Polycrystalline graphene by CVD

The earliest reports on CVD synthesized thin graphite materials were around 1970s in the early days of investigation into CVD process[13-15]. However, the first successful synthesis of few-layer graphene films of about 30 layers via CVD was reported by Somani et al. with nickel foils as substrates and camphor as gaseous reactant (**Figure 1a**)[8]. This work demonstrated the plausibility of CVD growth of layered graphene films, but there is much room for further reducing the thickness.

Chemical Science Accepted Manuscript

Following this work, many efforts have been made to optimize the CVD growth of graphene films, focusing on precursors, substrates, catalysts, temperatures and atmospheres. Reina et al. managed to reduced the layers of CVD synthesized graphene to few-layer level [16] . 500 nm Ni film was evaporated onto SiO_2/Si substrates as catalyst. After reductive annealing, few-layer graphene was deposited onto the substrates at 900-1000 ^oC with 5-25 sccm methane and 1500 sccm hydrogen as the gas flow at atmospheric pressure. The synthesized graphene consists of 1-12 layers with single or double layer regions of up to 20 μm. The prepared graphene film can withstand multiple processing steps without compromising the structural integrity. In another work, Pollard et al. demonstrated CVD growth of single-layer graphene on Ni thin film evaporated on SiO_2/Si substrates [17] . The Ni film was deposited onto SiO_2 (300 nm in thickness)/Si(100) substrates by sublimation under 10^{-4} – 10^{-5} Pa. Freestanding single-layer graphene film was obtained by etching off the Ni film.

One of the most important advances on CVD growth of single layer graphene was reported in 2009. Li et al. prepared large-area graphene film via CVD on copper foils,[18] and the grown graphene films were mostly of single-layer thickness, with less than 5% double or triple layers (**Figure 1b**) . Methane and hydrogen were applied as gas source in this work, and copper foil substrates were sequentially removed by treatment with iron nitrite solution to obtain free-standing graphene films. The chemical etching process to remove the substrates would become widely applied, since it took advantage of the chemical stability of graphene which avoided defects induced by micromechanical exfoliation and enabled easy transfer to dedicated substrates or films for heterostructure construction. To obtain uniform monolayer large area graphene, it is useful to selectively remove the bi-/tri- layer graphene. Fang et al. demonstrated bi-/tri-layer graphene was selectively removed by the carbon-absorbing enclosed W foil in Cu foil while the monolayer graphene remained intact[19].

Compared to single-layer graphene, bilayer graphene has a tunable bandgap which could benefit many electronic and optical device applications [20] . Lee et al. prepared wafer-scale bilayer graphene by CVD using methane [21] . The key factor in

Chemical Science Accepted Manuscript

this work is to control the cooling rate down to approximately 18Kmin^{-1}. The bilayer coverage is 99% , and the method is easy to scale up. Another route to synthesize bilayer graphene is epitaxial one layer graphene onto another layer. Yan et al. demonstrated a layer-by-layer vapor phase epitaxial synthesis of bilayer graphene [22] . A second layer of graphene was grown on copper foil which was already deposited with a layer of graphene. However, only 67% coverage of bilayer graphene was achieved and more efforts are needed.

Besides single or bilayer graphene, it is also important to gain control over the number of layers of CVD grown graphene. Gong et al. controlled the number of layers of CVD graphene within 1-10 layers mainly by controlling the flow of hydrogen, the thickness of deposited nickel catalyst, and growth temperature and time [23]. But to obtain uniform graphene with consistent number of layers is still challenging. In another work, by delicately controlling the parameters including temperature, deposition time, overall gas flow and pressure, control over the layers of CVD grown graphene were realized. Tu et al. took the control one step further with accuracy of down to one single layer within 7 layers [24] .

For the catalyzed CVD growth of graphene, complicated transfer from metal to working substrates are needed. Therefore, many efforts have been made to deposit graphene films onto the real working substrates without any catalysts. Shang et al. applied microwave-assisted plasma chemical vapor deposition (MPCVD) to grow multi-layered graphene on silicon substrates [25]. Hwang et al. synthesized single layer graphene on sapphire substrate via Van der Waals epitaxy by CVD [26] . Although the deposition temperature was around 1400°C, p-type and n-type single-layer graphene could be obtained by altering the partial pressure of methane gas. Wang et al. shows a slightly different work and the single layer graphene films were synthesized via CVD on h-BN films grown by CVD on copper foils [27]. Chen et al. demonstrated catalyst-free CVD growth of single crystal graphene on various dielectric substrates, such as $Si_3N_4/SiO_2/Si$ and sapphire [28]. The CVD growth was near-equilibrium, resulting in single crystal graphene sheets with quality close to metal-catalyzed sheets but with small sheet of only 11μm size.

Chemical Science Accepted Manuscript

Single crystal graphene by CVD

Most of the CVD synthesized graphene is polycrystalline graphene which shows much inferior performance compared to the exfoliated one from bulk graphite. It is believed that the grain boundaries in polycrystalline graphene are the main cause for the inferiority. Thus, many efforts have been devoted to the controllable and high-quality synthesis of single crystal graphene. The common approach is to modify the substrates / catalyst films, typically by annealing under hydrogen atmosphere at a higher temperature to promote grain growth and the suppression than a normal CVD growth. Larger grains will induce fewer grain boundaries thus enhanced performances. Applying single crystal substrates/catalyst films in the CVD growth of graphene would produce single crystal graphene [29], although the commercially-available single crystal substrates/catalyst films are too expensive for massive application.

Recently, CVD growth of single crystal graphene was successfully executed on commercial transitional metal substrates like copper foils. Vlassiouk et al. [7] grew large single crystal graphene via CVD process under an atmosphere of hydrogen, methane and argon with copper foils as substrates and catalyst, and hydrogen as a cocatalyst. By altering the partial pressure of hydrogen and methane, well-defined perfect single crystal graphene was obtained. The size of obtained graphene was around 10 μm, and the graphene showed weak binding to copper foil substrates, which benefits sequential removal of substrates and the fabrication of prototype devices. In another work, Wu et al. [30] managed to increase productivity of single crystal graphene on copper foils via CVD method by employing of PMMA dot arrays onto copper foils. The PMMA patterns were sequentially spin-coated, cured and annealed prior to a high temperature CVD process under atmosphere of argon, methane and hydrogen. By employing additional PMMA coating after CVD process, the arrangement of graphene grains was successfully kept uncompromised during the removal of copper foils and transfer process. The size of graphene grains was also around 10μm. Similarly, under atmospheric pressure, Robertson [31] and Warner

Chemical Science Accepted Manuscript

synthesized hexagonal single crystal graphene domains via CVD with copper as substrates and co-catalyst with hydrogen. The obtained graphene was single crystal few layer graphene.

Besides the productivity, increasing the size of grown graphene sheets is also a point of interest. Li et al. [32] further improve above-mentioned technical routes one step further. With low pressure and extended growth time of CVD process, Li et al. obtained graphene grain as large as 0.5 mm. Copper enclosure was used as substrates, offering a large deposition site for graphene. Wang et al. [33]also prepared single crystal graphene sheets with sub-millimeter size via an atmospheric pressure CVD (APCVD) process. Chen et al. suppressed evaporation loss of copper during CVD growth of single crystal graphene, and obtained graphene sheets with size up to 2 mm [34] . In their work, the CVD process was operated under low pressure, and if the deposition process lasted long enough, the copper substrate could suffer from evaporative loss during the deposition due to the high deposition temperature. Controlling chamber pressure can lead to single crystal CVD growth. Yan et al. [35] obtained single crystal graphene sheets with the size of 2.3 mm via a controlled chamber pressure CVD process. The chamber pressures of substrate and catalyst pre-deposition treatment, deposition and cooling procedure were all modified. Besides controlling the chamber pressure, manipulating carbon source could also trigger the growth of large size single crystal graphene. Gan et al. [36] prepared even bigger single crystal graphene sheets by delicately controlling the hydrogen flow throughout the process. The crucial step was to anneal the copper substrates under Ar atmosphere before the reductive pre-deposition treatment under Ar/H_2 atmosphere. The annealing induced mild oxidation, which provided unique nucleation sites or seeds for CVD growth of single crystal graphene. With prolonged deposition time, single crystal graphene sheets with size of up to 5.9 mm were obtained (**Figure 1c**). Zhou et al. also demonstrated the similar results [37]. They systematically studied argon atmosphere annealing before reductive heat treatment, low chamber pressure and high hydrogen/methane molar ratio of over 1000, and showed significantly reduced nucleation density in the CVD process. The size of resulting single crystal single-layer graphene sheets was 5 mm,

Chemical Science Accepted Manuscript

and the size of resulting single crystal double-layer graphene sheets was 300 μm. These works were all carried out on metal substrates. However, Lee et al. prepared wafer-scale monolayer single crystal graphene on epitaxial Ge film on silicon wafer as substrate [38] . The single crystal monolayer graphene can reach 2 inch wafer size.

The carbon precursors applied in above-mentioned works are gaseous methane, but it is not the only option. Wu et al. demonstrated that, by heating polystyrene with halon lamp, carbon source feedstock could easily be manipulated. Even with an atmospheric pressure CVD process, single crystal graphene with the size of up to 1.2 mm could be synthesized [39]. This work not only demonstrated the plausibility of modifying carbon source feedstock to obtain large single crystal graphene, but also revealed a new type of precursor other than gaseous methane. Xue et al. [40] also reported CVD growth of single crystal graphene with pyridine as precursor, which realized nitrogen doping during the synthesis. These kinds of CVD growth methods with non-gaseous precursors exhibit the advantage of significantly lower deposition temperature, but high-temperature pre-deposition treatment of substrates/catalysts are still necessary. Meanwhile, a direct indication and a precise control of the precursor flow is difficult to come by. Therefore, gaseous precursors like methane are still the most applied carbon source in the synthesis of single crystal graphene by CVD.

Most CVD process needs temperature below the melting point of copper. However, several works have been demonstrated with CVD reaction temperature above the melting point of copper, which would favor the growth of relatively large sheets of single crystal graphene. Wu et al. [41] raised deposition temperature to above the melting point of copper, and with Mo foils that could be wetted by copper as the substrates and melted copper as catalyst, sub-millimeter size single crystal graphene sheets was obtained via atmospheric pressure CVD. Geng et al. demonstrated CVD growth of smaller but denser single crystal graphene flakes. In their work, control over the size and productivity of single crystal graphene flakes was gained by controlling the temperature and partial pressure of methane gas flow [42]. Geng et al. demonstrated controlled CVD growth of twelve pointed graphene grains (TPGG) on a melted copper film with tungsten foils underneath as substrates(**Figure 1d**)[43]. The

Chemical Science Accepted Manuscript

as-synthesized TPGG was single crystal, and the morphology was controlled by altering the carbon feedstock. Melting and resolidifying substrates prior to CVD growth, would achieve similar effect as keeping the substrates molten. Mohsin et al. melted and resolidified copper film on tungsten substrates by sequential rising and reducing the temperature to obtain smooth surface and minimal surface irregularities[44]. The nucleation density was significantly reduced and CVD growth of graphene on this type of copper under high reaction temperature obtained millimeter sized single crystal graphene flakes with well defined hexagonal shape. The reductive treatment of copper was still necessary to suppress other irregularities in the copper catalyst.

Most single crystal graphene synthesized via CVD is single layer, especially the large-sized ones. CVD growth of large few-layer single crystal graphene is still a challenge. Yan et al. demonstrated CVD growth of double and triple layer graphene single crystals, in which the interlayer rotation within graphene single crystals were induced by graphene nucleation on copper foils steps during the synthesis [45] . The pre CVD treatment were prolonged to 7 hours in order to achieve the required copper surfaces. In **Table 1**, we summarize substrates, catalysts, overall gas flows, temperatures, pressures and corresponding product quality of graphene for some typical CVD growth processes.

Mechanism insight in CVD growth of single crystal graphene

CVD growth of single and polycrystalline graphene are two kinds of procedures that are similar in many aspects (**Figure 2a**)[35]. However, there are several key factors that distinguish the CVD growth of single crystal graphene[46]. First, suppression of nucleation allows space for the growth of single crystal graphene. The pre-deposition, reductive treatment of typical substrates (copper) eliminates impurity, oxides, sharp wrinkles, defects and other structures of the substrates that could favor the nucleation of graphene. Second, by reducing the partial pressure of methane gas in the overall gas flow, the concentration of carbon precursors would be low enough to favor the growth of graphene single crystal over the nucleation. Third, the deposition

Chemical Science Accepted Manuscript

parameters should be controlled so the single crystal graphene grains would grow to a relatively large size, but not too large to stack over one another. The parameters include chamber pressure, temperature, heating and cooling discipline, deposition time and composition and flow rate of the overall gas flow.

Many investigations indicate the special role of oxygen in the CVD growth of single crystal graphene. Gan et al.'s work showed that by mild oxidation of copper substrate before reductive annealing, copper nanoparticles with proper size could be obtained (**Figure 2b**)[36]. The nanoparticles promoted nucleation and growth of large single crystal graphene sheets. In their work, the origin of oxidation was identified as the trace amount of oxygen in Ar gas flow or residue oxygen in the CVD chamber. A detailed investigation into the effect of oxygen during the CVD growth of graphene was performed by Hao et al. (**Figure 3**)[47]. Various concentrations of surface oxygen in copper substrates were realized by purchasing copper foils with different purity, altering hydrogen pressure during reductive treatment and exposure to pure oxygen before CVD growth. The studies showed that surface oxygen in copper substrates could decrease the concentration of copper active sites by passivation, and thus suppress nucleation, favoring the growth of single crystal graphene nanosheets. Magnuson et al. offered a new perspective on the role of oxygen and the oxidation process of copper substrates[48] . By intentionally oxidizing the copper substrates, a layer of copper oxides was formed, which would decompose during the following annealing and CVD process and the residual carbon of the substrates would be eliminated. And this kind of behavior was referred to as "self-cleaning". There is also excellent work of in-situ observation of CVD growth of graphene[49]. However, deeper understanding of oxygen in the process is still needed to understand the complete role and mechanism of oxygen and to achieve delicate control over the condition of oxygen.

CVD growth of 2D Boron nitride (BN)

III-V compound thin films have been the focus of artificially-synthesized

Chemical Science Accepted Manuscript

thin-film materials. Since 1970s, GaAs thin film has been widely studied via molecular beam epitaxy. Other III-V compounds such as BN have also attracted much interest of the scientific community. For crystalline BN, there are two types of crystallinity, cubic and hexagonal, and marked as c-BN and h-BN. C-BN exhibits several fascinating properties, hardness second only to diamond, high thermal conductivity, high chemical stability and wide bandgap. In the early time of research on crystalline BN, much effort was focused on c-BN. H-BN is a relatively new type of material, consisting of sp2-bonded hexagons like graphite. H-BN exhibits high electrical resistivity, high thermal conductivity, extremely low dielectric constant and outstanding lubrication and anti-corrosion properties. It is vital to effectively control the crystallographic phase of obtained BN films, which could benefit future applications. However, due to the high cost of molecular beam epitaxy BN, CVD is introduced to lower the cost and promote the massive production. BN is very suitable for CVD growth since the precursors of B and N are mostly gaseous sources.

Pieson's work could be among the earliest study on synthesizing BN via CVD [50] . The deposition was carried out in a vertically set CVD device, with BF_3 and NH_3 as precursors of B and N, respectively. The deposition took place on BN felt fiber substrates at temperatures of 1100 ^oC to 1200 ^oC, demonstrating the plausibility of synthesizing BN via CVD. However, BN was deposited homogeneously on BN substrates, limiting the applications of CVD BN. For heterogeneous synthesis, Yamaguchi et al. demonstrated CVD grown BN on non-BN substrates for the first time [51]. In details, comparative stoichiometric BN films were grown on InP substrates via CVD with B_2H_6 and NH_3 as precursors of B and N, respectively. By introducing PH_3 into the overall gas flow, the doping of BN with P was also realized. P-doped BN films on InP substrates were readily applied as gate insulation. Similar work by Nakamura et al. showed that the composition of BN films synthesized by CVD could be closely controlled by varying the partial pressures of respective gaseous precursors [52]. In addition, various routes of CVD growth to obtain BN were demonstrated, including MOCVD [53] with $(C_2H_5)_3B$ and NH_3 gaseous precursors, microwave PECVD [54] with $NaBH_4$, NH_3 and H_2 precursors, and single precursor CVD process [55]

Chemical Science Accepted Manuscript

with polymeric cyanoborane precursor. These early works on the CVD growth of BN opened up the field and set the foundation of following CVD 2D BN nanosheets.

Several works have demonstrated CVD growth of 2D BN thin films. For example, Shi et al. demonstrated CVD growth of h-BN thin films with thickness of a few to tens of nanometers (**Figure 4a**)[56]. In this work, the h-BN thin films were deposited with an APCVD system, in which polycrystalline Ni was exposed to borazine vapor diluted in N_2 gas flow. By controlling the deposition temperature, a polymerization reaction took place to form polyborazylene, which could be further dehydrogenated to form h-BN with few layers. Similar work by Song et al. demonstrated large-scale CVD growth of high-quality h-BN films consisting of 2 to 5 atomic layers [57]. Ammonia borane (NH_3-BH_3) was applied as precursors of BN, and was carried along by a gas flow of Ar/H_2 (15% vol H_2, 85% vol Ar). The deposition was done at a temperature of around 1000 ^{o}C with a typical growth time of 30 -60 minutes.

Growing single layer BN films on various substrates requires more delicate control over the synthesis parameters, such as precursors, temperatures, content and flow rate of the overall gas flow, and chamber pressures[58]. Auwarter et al. demonstrated CVD growth of single layer BN on Ni (111) with B-trichloroborazine as a single precursor [59]. The deposition process was pretty straightforward, but required a rather sophisticated pre-deposition treatment of Ni (111) substrates to eliminate irregularities and a delicate control over the overall gas flow due to the sensitive nature of the B-trichloroborazine precursor. Several works also have demonstrated CVD growth of single layer BN on single crystal transitional metal substrates such as Au(111), Ru(001), Rh(111), and Pt(111) [60-64] . These works were carried out via ultra high vacuum chemical vapor deposition (UHVCVD). Considering the high growth rate of BN, it is difficult to grow single layer BN films, while UHVCVD could lower the growth rate and favor the growth of single layer BN with low concentration of precursors. Uniformly APCVD or LPCVD growth of single layer BN is also difficult due to the high deposition rate, and the resulting films consist of multiple-layer domains [65] . For a typical LPCVD growth of single layer BN [66] , the growth was

Chemical Science Accepted Manuscript

carried out at a temperature of 1100 ^{o}C under a constant pressure of 0.1 Torr with decomposed ammonia borane as gaseous precursors. Kim et al. employed an alternative single source to provide precursors [67] . Borazane powder was decomposed to produce BN precursor and the deposition was achieved on Cu substrates at a lower temperature under a pressure of 350 mTorr. Based on the understanding of the deposition process, Gao et al. developed a new route to gain control over the number of BN layers during APCVD growth [68]. Park et al. demonstrated an LPCVD process that resulted in large-area monolayer BN. [69] At a pressure of below 0.1 Torr, large area monolayer BN was obtained using cleaned, annealed Pt as substrates and borazine bubbled by hydrogen as precursor,.

In the typical APCVD process, vaporized borazane carried by Ar was mixed with an Ar/H_2 mixture to form the overall reactive gas flow, and a filter was introduced in the upstream of the deposition site to eliminate BN nanoparticles from thermal decomposition of borazane. By altering the concentration of borazane in the overall gas flow, selective monolayer, bilayer and few-layer BN growth was realized.

Growing single crystal BN nanosheets via CVD is still a big challenge and more efforts are obviously required. In one work, Gao et al. achieve individual single/ double layer BN domains by altering deposition time and concentration of precursor (vaporized borazane) (**Figure 4b**)[68]. The size of individual BN domains was around 1 µm, and demonstrated the possibility to obtain single crystal sheets by controlling the growth process. In another study, Wang et al. tried to regulate the nucleation process in the beginning of CVD growth (**Figure 4c**)[70]. The density of nucleation was significantly reduced by thoroughly annealing Cu substrates under the reductive atmosphere (at 1050°C for up to 6 hours) with ammonia borane as precursor. BN single crystal sheets with size of up to 20µm were normally observed. Larger grains mean fewer domain boundaries and lead to better performance in the future application of devices.

Chemical Science Accepted Manuscript

CVDgrowth of2DTransitional metal dichalcogenides

TMDs are fundamentally and technologically intriguing due to the unique electronic and optical properties. The properties of TMDs are versatile, ranging from insulators, semiconductors, true metals to superconductors. Reducing the stacking of TMDs to atomic layers leads to new characteristics induced by quantum confinement effects. Similar with graphene, single- and few- layer 2D TMD nanosheets can be obtained from either top-down routes like mechanical exfoliation or bottom-up process like chemical vapor deposition (CVD) . The focuses of CVD growth of TMDs are to grow few- and single- layer sheets, and to prepare single crystal TMDs atomic layers. Atomic layer control offers controlled properties and single crystal atomic layers result in better performance over their polycrystalline counterparts in many device applications.

CVD growth of TMD could date back to 1988 when Hofmann demonstrated MOCVD growth of MoS_2 and WS_2 on various substrates [71]. In this early work, MoS_2 and WS_2 were grown on various substrates, such as insulators/optical materials (glass, quartz, LiF, MgO and mica), transitional metals and noble metals/ conductors (Mo, Au, Pt, Al, Cu and steel). The precursors of Mo and W were hexacarbonyls of the corresponding transitional metal and the precursor of S was vaporized sulfur or hydrogen sulfide gas. However, the films are normally thick. To prepare two dimensional atomic layers or single layer, several techniques in CVD have been developed. Liu et al. reported a two-step thermolysis process,[72] in which ammonium thiomolybdates [$(NH_4)_2MoS_4$] were dip-coated onto the substrates, and were converted to MoS_2 by annealing at 500 ^oC under Ar/H_2 atmosphere followed by sulfurization at 1000 ^oC by sulfur vapor along with Ar gas. High-resolution TEM analysis identified that the MoS_2 is of three layer thickness, and the MoS_2 films could be easily transferred onto other arbitrary substrates. The sulfurization process with S vapor drastically enhanced the crystallinity of MoS_2.In another work, few layer TMDs could be obtained through conventional CVD process. Zhan et al. reported CVD growth of large-area MoS_2 few-layer atomic layers based on the sulfurization of Mo

Chemical Science Accepted Manuscript

metal films (**Figure 5a**)[73]. A thin layer of Mo was deposited on SiO_2 by electronic beam evaporator before placed in the tube furnace for CVD growth. Sulfur vapor was introduced into the process by heating the sulfur powder. The size of grown MoS_2 depended on the size of the substrates, and the thickness of MoS_2 depended on the thickness of Mo films deposited on the substrates.

Besides elemental precursors, transitional metal oxides could also be applied as the precursors. For example, Lee et al. synthesized few-layer MoS_2 by CVD [74] . In this work, MoO_3 was converted to MoS_2 by sulfurization. The pre-deposition treatments of substrates like SiO_2 with aromatic molecules were applied to assist the growth of MoS_2 atomic layers. However, in this work, full coverage of the substrates remains challenging. Liu et al. demonstrated a more delicate version of this technique [75] , where three-zone tube furnace with a much longer zone and stable temperature were required and the distance between sulfur and MoO_3 could be adjusted without compromising the temperature zone (**Figure 5b**). The as-synthesized MoS_2 exhibits strong capability in gas and chemical sensing applications. Najmaei et al. modified this route further by hydrothermally synthesizing MoO_3 nanoribbons as precursors of Mo [76] . By altering the amount of MoO_3 nanoribbons dispersed onto the substrates, control over Mo precursors and the resulted atomic layers were realized. McCreary et al. grew monolayer MoS_2 film on graphene substrate [19] . In this study, the precursor for Mo was $MoCl_5$ which was different from most other works, andMoS_2 films with 1, 2 or 3 layers were obtained by altering the amount of $MoCl_5$.Huang et al. prepared large area monolayer WSe_2 on sapphire substrates by CVD with WO_3 and Se applied as corresponding precursors.[38]The CVD process was carried out under mixed gas flow of Ar and H_2, which would assist the activation of the reactions between Se and WO_3. At a relatively low temperature of 750°C, continuous monolayer film of WSe_2 was obtained.

CVD growth of single crystal TMDs is still a big challenge to date, and the obtained single crystal TMD flakes or domains to date are relatively small compared to single crystal graphene flakes. However, some success in CVD growth of single crystal TMDs with large domain sizes has been realized recently. To grow single

Chemical Science Accepted Manuscript

crystal TMDs, the main solutions are still to reduce nucleation density to form larger domains/grains, and to control the growth process to obtain individual domains that form fewer or no domain boundaries. Laskar et al. demonstrated CVD growth of large area single crystal MoS_2 with (0001) orientation [77], where single crystal Al_2O_3 was applied as the substrate . The overall CVD process was basically the sulfurization of evaporated Mo thin film by sulfur vapor. By tuning the sulfurization time, high quality MoS_2 films were obtained and was confirmed by planar view selective area diffraction patterns. However, the resulted films are relatively thick hindering the further applications.

Besides elemental Mo and S, MoO_3 and S could also be applied as precursors for CVD growth of single crystal MoS_2.Wang et al. demonstrated layer-by-layer sulfurization CVD growth of single crystal MoS_2 flakes[78]. The process was based on the conversion of MoO_3 to MoS_2 by sulfurization with vaporized S. Some MnO_2 was introduced into the process to react with excess sulfur. It should also be noted that the substrates were placed downstream of MoO_3 rather than on top of it as in most cases. By controlling the deposition parameters, the layers of obtained highly oriented MoS_2 flakes could be controllable tuned from single, double, triple to quadruple layers. Van der Zande et al. prepared monolayer single crystal MoS_2 nanosheets with size of up to 120μm via CVD growth[79] . The process was carried out under atmospheric pressure in a N_2 gas flow, and a high yield was obtained with ultra clean substrates and fresh precursors.

The process could be applied to other TMDs as well. Zhang et al. demonstrated CVD growth of monolayer single crystal WS_2 nanosheets on single crystal sapphire substrates with WO_3 and S as precursors [80] . The synthesis process was carried out under low pressure at a temperature of ~900°C for ~60 minutes and the product was monolayer single crystal WS_2 nanosheets with size up to 50 μm.Rong et al. demonstrated CVD growth of large single crystal domains of WS_2 (**Figure 5c**)[81]. By controlling the time and amount of sulfur introduced before and during the CVD process, monolayer WS_2 domains with sizes of up to 370 μm were obtained, which was visible to naked eye. The pre-deposition treatment of WO_3 with sulfur was

Chemical Science Accepted Manuscript

realized by heating the sulfur 15 minutes before the WO_3 was heated up to the designated temperature for the CVD process. It should also be noticed that, by loading aromatic molecules onto the substrates as seeding promoters, synthesis of large monolayer single crystal TMDs is favored. For example, Ling et al. demonstrated that the favored growth of large single crystal TMD monolayer with a substrate loaded with seeding promoters.[82]

Besides the TMD materials mentioned above, heterostructures based on TMD materials are attracting great interest. First principle calculation of band offset predicted that certain kinds of TMD monolayers based heterostructures with type-II band alignment would be suitable for applications in the fields of photovoltaics, optoelectronics and energy conversion and storage [83] . Other than type-II band alignments, heterostructures based on single-layer TMD and graphene with Schottky barriers were also investigated by theoretical calculations. Bernardi et al. have theoretically demonstrated that bilayer solar cells of MoS_2/graphene of 1 nm thickness could achieve over 1% power conversion efficiency [84]. These theoretical works predicted that bilayers of TMD/TMD or TMD/graphene could be promising in various fields of applications. There are several experimental works on TMDs based heterostructures. Huang et al. demonstrated lateral heterostructures within single layer $MoSe_2$-WSe_2 material [85] . The synthesis process was vaporizing and deposition of a mixture of $MoSe_2$ and WSe_2 with high purity H_2 working as carrier gas (**Figure 6**). Duan et al. developed a CVD system that allowed in-situ switch of solid sources [86] . By sequentially vaporizing and depositing WS_2 and WSe_2, WS_2-WSe_2 lateral heterostructures were obtained under high temperature, atmospheric pressure and vigorous Ar flow. Furthermore, Duan et al. also demonstrated synthesis of single to few layer MoS_2-$MoSe_2$ lateral heterostructures using the same system. MoO_3 was applied as precursor of Mo, when S and Se powders were sequentially vaporized and reacted with MoO_3 to obtain MoS_2-$MoSe_2$ lateral heterostructures. Similarly, Zhang et al. demonstrated CVD synthesis of TMD lateral heterostructures by sequential CVD synthesis of corresponding TMDs.[87]

Chemical Science Accepted Manuscript

Conclusion and perspective

We have briefly reviewed the CVD growth of two-dimensional materials, focusing on three types of signature 2D materials, graphene, BN and TMDs. The preparation process and fundamental growth mechanism of CVD growth, from few and single layer films to single crystal atomic sheets, are discussed. Substantial progress has been made in understanding the influence of growth parameters, including precursors, substrates, atmospheres and gas flows.

The development in CVD growth of 2D materials is driven by the growing demand of high quality 2D materials in various fields of applications where full control of CVD growth is critical. However, such full control over the CVD growth process is still yet to be achieved. Complete understanding of the impact of growth parameters has special importance to realize the programmable control of CVD growth and the high quality of grown 2D materials. For example, the synthesis of larger single crystal 2D materials with the quality comparable with mechanical exfoliation is still a big challenge. As for the CVD process, the key factors for larger single crystal 2D materials are suppression of nucleation and well-maintained growth. Suppression of nucleation could be realized by thoroughly cleaning and smoothing the substrates, lowering the concentration of precursors, and carrying out the process at a higher temperature. Well-maintained growth process could be achieved by an optimized temperature, pressure and gas flow where slow growth may need longer growth time than usual growth. In addition to the larger single crystal 2D materials, controllable CVD growth of heterostructures based on 2D materials and integration of CVD growth of 2D materials with device fabrication are highly expected in the near future.

Chemical Science Accepted Manuscript

Jingxue Yu is a postdoctoral research fellow at Huazhong University of Science & Technology. He received his BS and doctoral degrees in materials science & engineering at Zhejiang University. Current research interests include synthesis and applications of graphene.

Jie Li is a Ph.D. candidate in the Department of Materials Science and Engineering at Huazhong University. He graduated from Shandong University of Technology in 2014. His current research focuses on the preparation and application of two-dimensional materials, especially for Transition metal dichalcogenides (TMDs)

Wenfeng Zhang is currently an associate Professor in School of Materials Science and Engineering, Huazhong University of Science and Technology (HUST), China. He received the Ph.D. degree from City University of Hong Kong, Hong Kong, China, in 2009.Then he worked in City University of Hong Kong, and the University of Tokyo as a postdoctoral researcher before he moved to HUST. His current research interests focus on the post-silicon semiconductor materials and devices, including graphene, transition metal dichalcogenides (TMDs), germanium and III-V

Chemical Science Accepted Manuscript

semiconductors etc.

Haixin Chang is a full Professor in School of Materials Science and Engineering, Huazhong University of Science and Technology, China. He got his Ph.D. in Materials Science in 2007 from Institute of Metal Research, Chinese Academy of Sciences. Then he worked in Department of Chemistry, Tsinghua University and Nanotechnology Centre, ITC, Hong Kong Polytechnic University before moving to Tohoku University in 2011. He was an Assistant Professor in WPI-AIMR, Tohoku University from 2012 to 2014. He received several awards such as National Thousands Talents Youth Award and Pulickel M. Ajayan Award. His researches cover broad topics of quantum nanomaterials and devices, with a recent focus on the synthesis, property, low-dimensional physics, and electronic, optoelectronic and energy devices based on graphene, transition metal dichalcogenides (TMDs) and other two-dimensional and quantum materials.

Acknowledgements

This work is supported by the National Basic Research Program of China (No. 2015CB258400), Natural Science Foundation of China (No. 51402118) and HUST.

Chemical Science Accepted Manuscript

References

1. A. De Lodyguine, US Patents, 1897.
2. R. Platz and S. Wagner, *Appl. Phys. Lett.*, 1998, **73**, 1236-1238.
3. K. L. Choy, *Prog. Mater. Sci.*, 2003, **48**, 57-170.
4. K. S. Novoselov, A. K. Geim, S. V. Morozov, D. Jiang, Y. Zhang, S. V. Dubonos, I. V. Grigorieva and A. A. Firsov, *Science*, 2004, **306**, 666-669.
5. E. S. Penev, V. I. Artyukhov, F. Ding and B. I. Yakobson, *Adv. Mater.*, 2012, **24**, 4956-4976.
6. X. Zhang, H. Li and F. Ding, *Adv. Mater.*, 2014, **26**, 5488-5495.
7. I. Vlassiouk, M. Regmi, P. Fulvio, S. Dai, P. Datskos, G. Eres and S. Smirnov, *ACS Nano*, 2011, **5**, 6069-6076.
8. P. R. Somani, S. P. Somani and M. Umeno, *Chem. Phys. Lett.*, 2006, **430**, 56-59.
9. W. Feng, S. Lei, Q. Li and A. Zhao, *The Journal of Physical Chemistry C*, 2011, **115**, 24858-24864.
10. T. Gao, S. Xie, Y. Gao, M. Liu, Y. Chen, Y. Zhang and Z. Liu, *ACS Nano*, 2011, **5**, 9194-9201.
11. C.-M. Seah, S.-P. Chai and A. R. Mohamed, *Carbon*, 2014, **70**, 1-21.
12. X. Li, W. Cai, L. Colombo and R. S. Ruoff, *Nano Lett.*, 2009, **9**, 4268-4272.
13. M. Eizenberg and J. Blakely, *Surf. Sci.*, 1979, **82**, 228-236.
14. J. Shelton, H. Patil and J. Blakely, *Surf. Sci.*, 1974, **43**, 493-520.
15. J. W. May, *Surf. Sci.*, 1969, **17**, 267-270.
16. A. Reina, X. Jia, J. Ho, D. Nezich, H. Son, V. Bulovic, M. S. Dresselhaus and J. Kong, *Nano Lett.*, 2009, **9**, 30-35.
17. A. J. Pollard, R. R. Nair, S. N. Sabki, C. R. Staddon, L. M. A. Perdigao, C. H. Hsu, J. M. Garfitt, S. Gangopadhyay, H. F. Gleeson, A. K. Geim and P. H. Beton, *The Journal of Physical Chemistry C*, 2009, **113**, 16565-16567.
18. X. S. Li, W. W. Cai, J. H. An, S. Kim, J. Nah, D. X. Yang, R. Piner, A. Velamakanni, I. Jung, E. Tutuc, S. K. Banerjee, L. Colombo and R. S. Ruoff, *Science*, 2009, **324**, 1312-1314.
19. W. Fang, A. Hsu, Y. C. Shin, A. Liao, S. Huang, Y. Song, X. Ling, M. S. Dresselhaus, T. Palacios and J. Kong, *Nanoscale*, 2015, **7**, 4929-4934.
20. A. Ramasubramaniam, D. Naveh and E. Towe, *Nano Lett.*, 2011, **11**, 1070-1075.
21. S. Lee, K. Lee and Z. Zhong, *Nano Lett.*, 2010, **10**, 4702-4707.
22. K. Yan, H. Peng, Y. Zhou, H. Li and Z. Liu, *Nano Lett.*, 2011, **11**, 1106-1110.
23. Y. Gong, X. Zhang, G. Liu, L. Wu, X. Geng, M. Long, X. Cao, Y. Guo, W. Li, J. Xu, M. Sun, L. Lu and L. Liu, *Adv. Funct. Mater.*, 2012, **22**, 3153-3159.
24. Z. Tu, Z. Liu, Y. Li, F. Yang, L. Zhang, Z. Zhao, C. Xu, S. Wu, H. Liu, H. Yang and P. Richard, *Carbon*, 2014, **73**, 252-258.
25. N. G. Shang, P. Papakonstantinou, M. McMullan, M. Chu, A. Stamboulis, A. Potenza, S. S. Dhesi and H. Marchetto, *Adv. Funct. Mater.*, 2008, **18**, 3506-3514.
26. J. Hwang, M. Kim, D. Campbell, H. A. Alsalman, J. Y. Kwak, S. Shivaraman, A. R. Woll, A. K. Singh, R. G. Hennig, S. Gorantla, M. H. Rümmeli and M. G. Spencer, *ACS Nano*, 2012, **7**, 385-395.
27. M. Wang, S. K. Jang, W.-J. Jang, M. Kim, S.-Y. Park, S.-W. Kim, S.-J. Kahng, J.-Y. Choi, R. S. Ruoff, Y. J. Song and S. Lee, *Adv. Mater.*, 2013, **25**, 2746-2752.
28. J. Chen, Y. Guo, L. Jiang, Z. Xu, L. Huang, Y. Xue, D. Geng, B. Wu, W. Hu, G. Yu and Y. Liu, *Adv.*

Chemical Science Accepted Manuscript

Mater., 2014, **26**, 1348-1353.
29. L. Gao, W. Ren, H. Xu, L. Jin, Z. Wang, T. Ma, L.-P. Ma, Z. Zhang, Q. Fu, L.-M. Peng, X. Bao and H.-M. Cheng, *Nat Commun*, 2012, **3**, 699.
30. W. Wu, L. A. Jauregui, Z. Su, Z. Liu, J. Bao, Y. P. Chen and Q. Yu, *Adv. Mater.*, 2011, **23**, 4898-4903.
31. A. W. Robertson and J. H. Warner, *Nano Lett.*, 2011, **11**, 1182-1189.
32. X. Li, C. W. Magnuson, A. Venugopal, R. M. Tromp, J. B. Hannon, E. M. Vogel, L. Colombo and R. S. Ruoff, *J. Am. Chem. Soc.*, 2011, **133**, 2816-2819.
33. H. Wang, G. Wang, P. Bao, S. Yang, W. Zhu, X. Xie and W.-J. Zhang, *J. Am. Chem. Soc.*, 2012, **134**, 3627-3630.
34. S. Chen, H. Ji, H. Chou, Q. Li, H. Li, J. W. Suk, R. Piner, L. Liao, W. Cai and R. S. Ruoff, *Adv. Mater.*, 2013, **25**, 2062-2065.
35. Z. Yan, J. Lin, Z. Peng, Z. Sun, Y. Zhu, L. Li, C. Xiang, E. L. Samuel, C. Kittrell and J. M. Tour, *ACS Nano*, 2012, **6**, 9110-9117.
36. L. Gan and Z. Luo, *ACS Nano*, 2013, **7**, 9480-9488.
37. H. Zhou, W. J. Yu, L. Liu, R. Cheng, Y. Chen, X. Huang, Y. Liu, Y. Wang, Y. Huang and X. Duan, *Nat Commun*, 2013, **4**.
38. J.-H. Lee, E. K. Lee, W.-J. Joo, Y. Jang, B.-S. Kim, J. Y. Lim, S.-H. Choi, S. J. Ahn, J. R. Ahn, M.-H. Park, C.-W. Yang, B. L. Choi, S.-W. Hwang and D. Whang, *Science*, 2014, **344**, 286-289.
39. T. Wu, G. Ding, H. Shen, H. Wang, L. Sun, D. Jiang, X. Xie and M. Jiang, *Adv. Funct. Mater.*, 2013, **23**, 198-203.
40. Y. Xue, B. Wu, L. Jiang, Y. Guo, L. Huang, J. Chen, J. Tan, D. Geng, B. Luo, W. Hu, G. Yu and Y. Liu, *J. Am. Chem. Soc.*, 2012, **134**, 11060-11063.
41. Y. A. Wu, Y. Fan, S. Speller, G. L. Creeth, J. T. Sadowski, K. He, A. W. Robertson, C. S. Allen and J. H. Warner, *ACS Nano*, 2012, **6**, 5010-5017.
42. D. Geng, B. Wu, Y. Guo, L. Huang, Y. Xue, J. Chen, G. Yu, L. Jiang, W. Hu and Y. Liu, *Proc. Natl. Acad. Sci.*, 2012, **109**, 7992-7996.
43. D. Geng, L. Meng, B. Chen, E. Gao, W. Yan, H. Yan, B. Luo, J. Xu, H. Wang, Z. Mao, Z. Xu, L. He, Z. Zhang, L. Peng and G. Yu, *Adv. Mater.*, 2014, **26**, 6423-6429.
44. A. Mohsin, L. Liu, P. Liu, W. Deng, I. N. Ivanov, G. Li, O. E. Dyck, G. Duscher, J. R. Dunlap, K. Xiao and G. Gu, *ACS Nano*, 2013, **7**, 8924-8931.
45. Z. Yan, Y. Liu, L. Ju, Z. Peng, J. Lin, G. Wang, H. Zhou, C. Xiang, E. L. G. Samuel, C. Kittrell, V. I. Artyukhov, F. Wang, B. I. Yakobson and J. M. Tour, *Angew. Chem. Int. Ed.*, 2014, **53**, 1565-1569.
46. H. Mehdipour and K. Ostrikov, *ACS Nano*, 2012, **6**, 10276-10286.
47. Y. Hao, M. S. Bharathi, L. Wang, Y. Liu, H. Chen, S. Nie, X. Wang, H. Chou, C. Tan, B. Fallahazad, H. Ramanarayan, C. W. Magnuson, E. Tutuc, B. I. Yakobson, K. F. McCarty, Y.-W. Zhang, P. Kim, J. Hone, L. Colombo and R. S. Ruoff, *Science*, 2013, **342**, 720-723.
48. C. W. Magnuson, X. Kong, H. Ji, C. Tan, H. Li, R. Piner, C. A. Ventrice, Jr. and R. S. Ruoff, *J. Mater. Res.*, 2014, **29**, 403-409.
49. Z.-J. Wang, G. Weinberg, Q. Zhang, T. Lunkenbein, A. Klein-Hoffmann, M. Kurnatowska, M. Plodinec, Q. Li, L. Chi, R. Schloegl and M.-G. Willinger, *ACS Nano*, 2015, **9**, 1506-1519.
50. H. O. Pierson, *J. Compos. Mater.*, 1975, **9**, 228-240.
51. E. Yamaguchi and M. Minakata, *J. Appl. Phys.*, 1984, **55**, 3098-3102.

Chemical Science Accepted Manuscript

52. K. Nakamura, *J. Electrochem. Soc.*, 1985, **132**, 1757-1762.
53. K. Nakamura, *J. Electrochem. Soc.*, 1986, **133**, 1120-1123.
54. H. Saitoh and W. A. Yarbrough, *Appl. Phys. Lett.*, 1991, **58**, 2482-2484.
55. L. Maya and H. L. Richards, *J. Am. Ceram. Soc.*, 1991, **74**, 406-409.
56. Y. Shi, C. Hamsen, X. Jia, K. K. Kim, A. Reina, M. Hofmann, A. L. Hsu, K. Zhang, H. Li, Z.-Y. Juang, M. S. Dresselhaus, L.-J. Li and J. Kong, *Nano Lett.*, 2010, **10**, 4134-4139.
57. L. Song, L. Ci, H. Lu, P. B. Sorokin, C. Jin, J. Ni, A. G. Kvashnin, D. G. Kvashnin, J. Lou, B. I. Yakobson and P. M. Ajayan, *Nano Lett.*, 2010, **10**, 3209-3215.
58. M. Corso, W. Auwärter, M. Muntwiler, A. Tamai, T. Greber and J. Osterwalder, *Science*, 2004, **303**, 217-220.
59. W. Auwärter, H. U. Suter, H. Sachdev and T. Greber, *Chem. Mater.*, 2003, **16**, 343-345.
60. R. J. Simonson, M. T. Paffett, M. E. Jones and B. E. Koel, *Surf. Sci.*, 1991, **254**, 29-44.
61. M. T. Paffett, R. J. Simonson, P. Papin and R. T. Paine, *Surf. Sci.*, 1990, **232**, 286-296.
62. A. Nagashima, N. Tejima, Y. Gamou, T. Kawai and C. Oshima, *Phys. Rev. Lett.*, 1995, **75**, 3918-3921.
63. A. Preobrajenski, A. Vinogradov, M. Ng, E. Ćavar, R. Westerström, A. Mikkelsen, E. Lundgren and N. Mårtensson, *Physical Review B*, 2007, **75**, 245412.
64. P. Sutter, J. Lahiri, P. Albrecht and E. Sutter, *ACS Nano*, 2011, **5**, 7303-7309.
65. A. Ismach, H. Chou, D. A. Ferrer, Y. Wu, S. McDonnell, H. C. Floresca, A. Covacevich, C. Pope, R. Piner, M. J. Kim, R. M. Wallace, L. Colombo and R. S. Ruoff, *ACS Nano*, 2012, **6**, 6378-6385.
66. G. Kim, A. R. Jang, H. Y. Jeong, Z. Lee, D. J. Kang and H. S. Shin, *Nano Lett.*, 2013, **13**, 1834-1839.
67. K. K. Kim, A. Hsu, X. Jia, S. M. Kim, Y. Shi, M. Hofmann, D. Nezich, J. F. Rodriguez-Nieva, M. Dresselhaus, T. Palacios and J. Kong, *Nano Lett.*, 2011, **12**, 161-166.
68. Y. Gao, W. Ren, T. Ma, Z. Liu, Y. Zhang, W.-B. Liu, L.-P. Ma, X. Ma and H.-M. Cheng, *ACS Nano*, 2013, **7**, 5199-5206.
69. J.-H. Park, J. C. Park, S. J. Yun, H. Kim, D. H. Luong, S. M. Kim, S. H. Choi, W. Yang, J. Kong, K. K. Kim and Y. H. Lee, *ACS Nano*, 2014, **8**, 8520-8528.
70. L. Wang, B. Wu, J. Chen, H. Liu, P. Hu and Y. Liu, *Adv. Mater.*, 2014, **26**, 1559-1564.
71. W. Hofmann, *J. Mater. Sci.*, 1988, **23**, 3981-3986.
72. K.-K. Liu, W. Zhang, Y.-H. Lee, Y.-C. Lin, M.-T. Chang, C.-Y. Su, C.-S. Chang, H. Li, Y. Shi, H. Zhang, C.-S. Lai and L.-J. Li, *Nano Lett.*, 2012, **12**, 1538-1544.
73. Y. Zhan, Z. Liu, S. Najmaei, P. M. Ajayan and J. Lou, *Small*, 2012, **8**, 966-971.
74. Y. H. Lee, X. Q. Zhang, W. Zhang, M. T. Chang, C. T. Lin, K. D. Chang, Y. C. Yu, J. T. Wang, C. S. Chang, L. J. Li and T. W. Lin, *Adv. Mater.*, 2012, **24**, 2320-2325.
75. B. Liu, L. Chen, G. Liu, A. N. Abbas, M. Fathi and C. Zhou, *ACS Nano*, 2014, **8**, 5304-5314.
76. S. Najmaei, Z. Liu, W. Zhou, X. Zou, G. Shi, S. Lei, B. I. Yakobson, J.-C. Idrobo, P. M. Ajayan and J. Lou, *Nat. Mater.*, 2013, **12**, 754-759.
77. M. R. Laskar, L. Ma, S. Kannappan, P. Sung Park, S. Krishnamoorthy, D. N. Nath, W. Lu, Y. Wu and S. Rajan, *Appl. Phys. Lett.*, 2013, **102**, 252108.
78. X. Wang, H. Feng, Y. Wu and L. Jiao, *J. Am. Chem. Soc.*, 2013, **135**, 5304-5307.
79. T. W. Myers, *Journal of Bodywork and Movement Therapies*, 1997, **1**, 135-145.
80. T. W. Myers, *Journal of Bodywork and Movement Therapies*, 1997, **1**, 91-101.
81. Y. Rong, Y. Fan, A. Leen Koh, A. W. Robertson, K. He, S. Wang, H. Tan, R. Sinclair and J. H.

Chemical Science Accepted Manuscript

Warner, *Nanoscale*, 2014, **6**, 12096-12103.

82. X. Ling, Y.-H. Lee, Y. Lin, W. Fang, L. Yu, M. S. Dresselhaus and J. Kong, *Nano Lett.*, 2014, **14**, 464-472.
83. J. Kang, S. Tongay, J. Zhou, J. Li and J. Wu, *Appl. Phys. Lett.*, 2013, **102**, -.
84. M. Bernardi, M. Palummo and J. C. Grossman, *Nano Lett.*, 2013, **13**, 3664-3670.
85. C. Huang, S. Wu, A. M. Sanchez, J. J. P. Peters, R. Beanland, J. S. Ross, P. Rivera, W. Yao, D. H. Cobden and X. Xu, *Nat. Mater.*, 2014, **13**, 1096-1101.
86. X. Duan, C. Wang, J. C. Shaw, R. Cheng, Y. Chen, H. Li, X. Wu, Y. Tang, Q. Zhang, A. Pan, J. Jiang, R. Yu, Y. Huang and X. Duan, *Nat Nano*, 2014, **9**, 1024-1030.
87. X.-Q. Zhang, C.-H. Lin, Y.-W. Tseng, K.-H. Huang and Y.-H. Lee, *Nano Lett.*, 2015, **15**, 410-415.

Chemical Science Accepted Manuscript

Figures& Tables

Table 1 The influence of CVD growth parameters on the quality of graphene.

Chemical Science Accepted Manuscript

Precursor	Special pre-deposition treatment of substrates	Substrates	Metal Catalyst	growth condition	Atmosphere & gas flow	Morphology	Properties	Remarks
Camphor	N/A	Ni	Ni	700-850°C	Atmospheric Pressure, Ar	Multi layer graphene film	N/A	Ref [8]
Methane	60 minutes, 40 mTorr, 2 sccm H_2, 1000°C	Cu	Cu	1000°C,30 min	~500mTorr, 2sccm H_2,35sccm CH_4	Single layer graphene films with no more than 5% domains of double or triple layer	Carrier mobility ~4050 $cm^2V^{-1}s^{-1}$	Ref [18]
Methane	900W nitrogen plasma 40 Torr several min	Si	N/A	Over 1000°C, 900-1300Wmicrowave	40 Torr, 10-40% methane in N_2	Multi layer graphene film	Fast electron-transper, selective electrocatalysis	Ref[25]
Methane	N/A	Sapphire	N/A	1450-1650°C, 45s-5min	600Torr, ~10000 sccm Ar, 5-200 sccmCH_4, H_2:CH_4=5-15	single layer graphene films	Carrier mobility ~2000 $cm^2V^{-1}s^{-1}$	Ref[26]
Methane	1180°C,30 min, 250 sccm H_2, 300 sccm Ar	Various dielectric materials	N/A	1180°C, 2 h	Atmospheric pressure CH_4:H_2=1.9~2.3:50 sccm	Single crystal hexagonal and dodecagonal up to 11um	Carrier mobility 5000 $cm^2V^{-1}s^{-1}$	Ref[28]

Chemical Science Accepted Manuscript

Methane	1040°C,10 minutes, 700 sccm H_2	Pt(111)	Pt	1040°C, 4 h	Atmospheric pressure, 4 sccm CH_4, 700 sccm H_2	Single crystal hexagonal graphene sheets of 1mm	Carrier mobility 7100 $cm^2V^{-1}s^{-1}$	Ref[29]
Methane	Chemical polishing, mild oxidation followed by reductive heat treatment	Cu	Cu	1050°C, up to tens of hours	Atmospheric pressure, 15 sccm 500 ppm CH_4 diluted in argon, 21 sccm H_2	Single crystal hexagonal graphene sheets of up to 5.9 mm	N/A	Ref[36]
Polystyrene, evaporated	Mechanical & chemical polishing, followed by reductive heat treatment	Cu	Cu	950-1050°C 30-80 min	Atmoshperic pressure, 300 sccm overall gas flow of Ar and H_2, 0-10 sccm H_2	Single crystal hexagonal graphene sheets of up to 1.2 mm	Carrier mobility 5000-8000 $cm^2V^{-1}s^{-1}$	Ref[39]
Pyridine, bubbled	Reductive heat treatment	Cu	Cu	300°C, 0.5-5 min	Atmospheric pressure, H_2:Ar=(150:30,100:20,50:10) sccm	Single crystal tetragonal graphene sheets	Nitrogen doped, Carrier mobility 53.5−72.9 $cm^2V^{-1}s^{-1}$	Ref[40]
Methane	Reductive heat treatment	Melted Cu on W	Cu	1120°C, 3-5 min	Atmospheric pressure, CH_4:H_2=3-5:300 sccm	Single crystal twelve pointed graphene sheets	Carrier mobility 2000-5000 $cm^2V^{-1}s^{-1}$	Ref[42]

Chemical Science Accepted Manuscript

Methane	Melting and resolidifying under reductive atmosphere	Resolidified Cu on W	Cu	1075°C, 5 h	Atmospheric pressure, CH_4:H_2:Ar=46:100:854sccm	Single crystal hexagonal graphene sheets of ~1mm	N/A	Ref[44]
Methane	Reductive heat treatment followed by oxygen exposure	Oxygen-rich Cu	Cu	1035°C, 30 min	CH_4, 5×10^{-3} Torr H_2, 0.1 Torr	Multi-branched graphene domains	Carrier mobility 15000-30000$cm^2V^{-1}s^{-1}$ at room temperature	Ref[47]

Chemical Science Accepted Manuscript

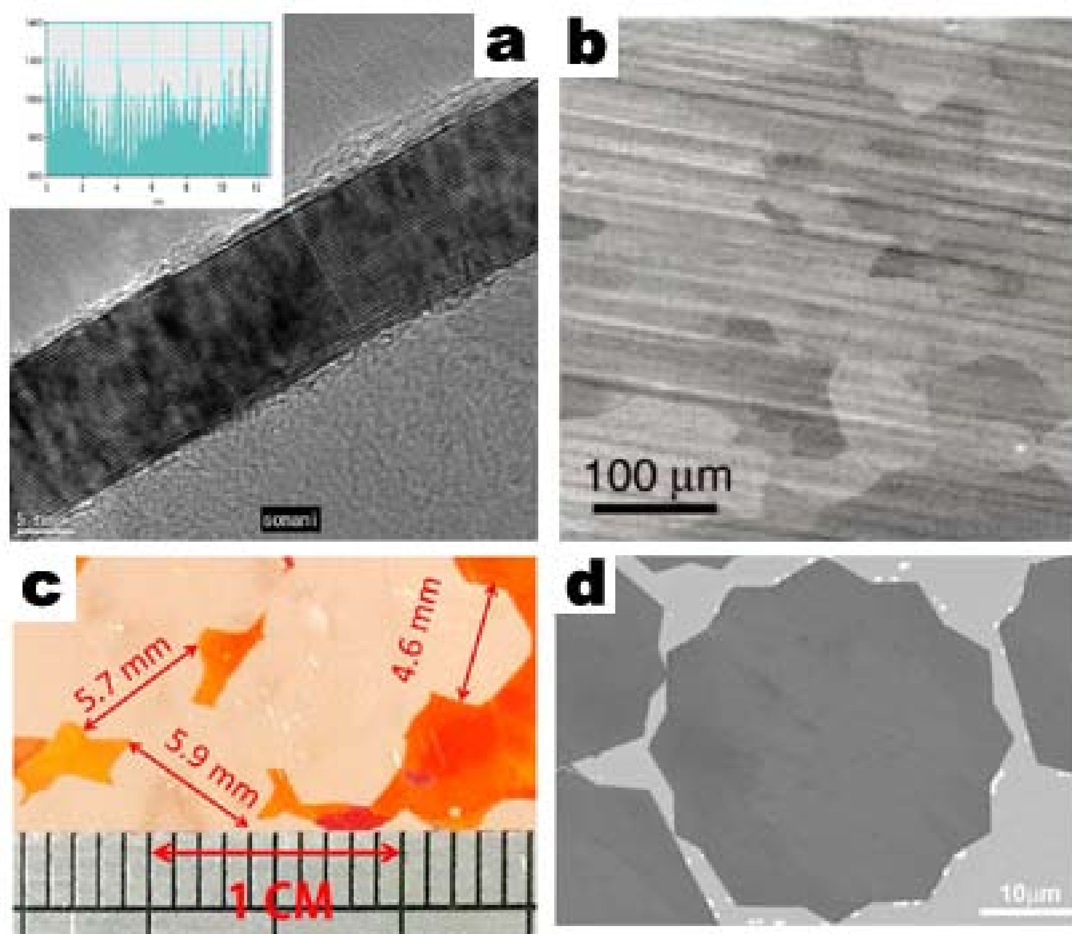

Figure 1. (a) TEM image of CVD synthesized graphene film, reprinted from ref[7] with permission by Elsevier; (b) SEM image of CVD synthesized single layer graphene film, reprinted from ref [18] with permission by American Association for the Advancement of Science; (c) Optical image of CVD synthesized single graphene sheets on copper foil, reprinted from ref[36]with permission by American Chemical Society; (d) SEM images of CVD synthesized single crystal twelve point graphene grain on melted copper, reprinted from ref[43] with permission by John Wiley & Sons.

Chemical Science Accepted Manuscript

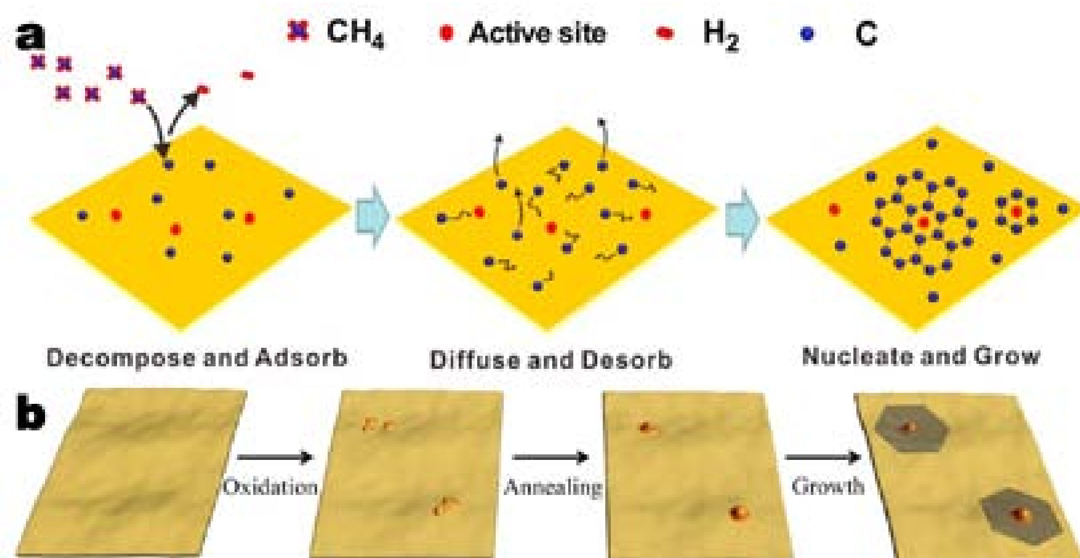

Figure 2. Schematic illustration for growth mechanisms of CVD growth process of graphene. (a) CVD growth process with methane precursor, reprinted from ref[35] with permission by American Chemical Society; (b) Scheme of the mild oxidation and sequential reductive heat treatment before CVD process, reprinted from ref[36] with permission by American Chemical Society.

Chemical Science Accepted Manuscript

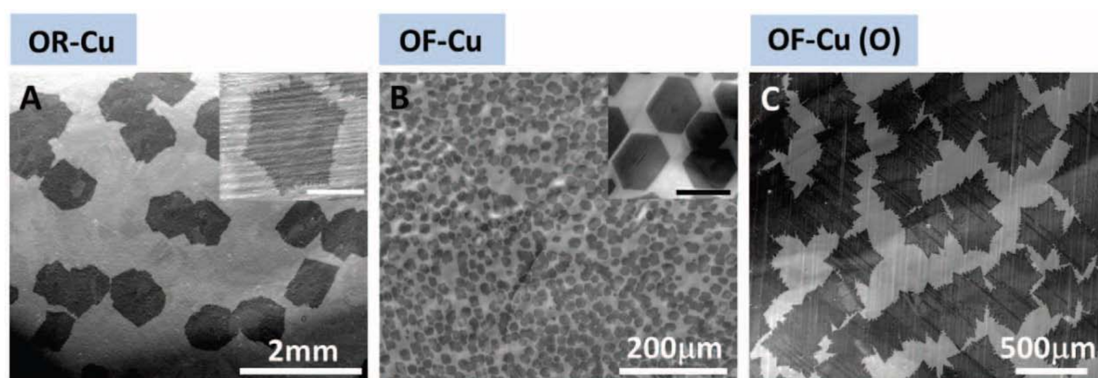

Figure 3.The effect of O on graphene nucleation density and domain shapes on various types of Cu substrates. OR-Cu represents low-purity copper substrates, OF-Cu represents high-purity copper substrates, and OF-Cu (O) represents high-purity copper substrates exposed to oxygen before CVD growth of graphene. Reprinted from Ref [47] with permission by American Association for the Advancement of Science

Chemical Science Accepted Manuscript

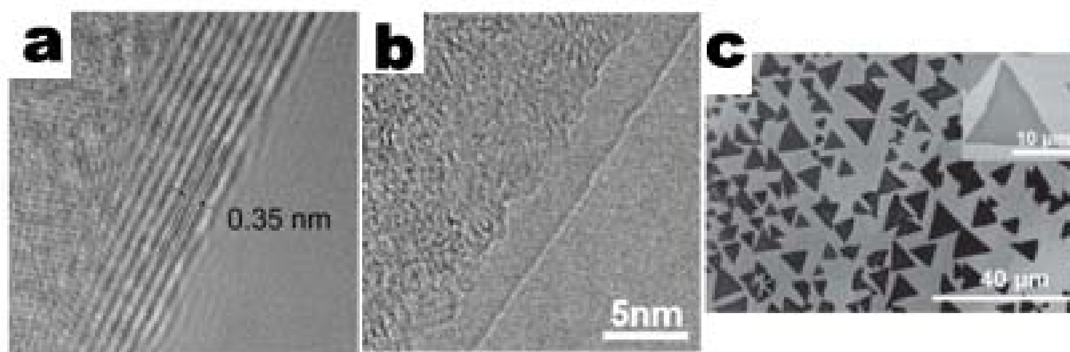

Figure 4. TEM image of few layer (a) and single layer (b) BN synthesized by CVD, reprinted from Ref[56] (a) and Ref[68] (b) with permission from American Chemical Society; SEM image of CVD synthesized single crystal BN (c),reprinted from Ref[70] with permission of John Wiley & Sons, Inc.

Chemical Science Accepted Manuscript

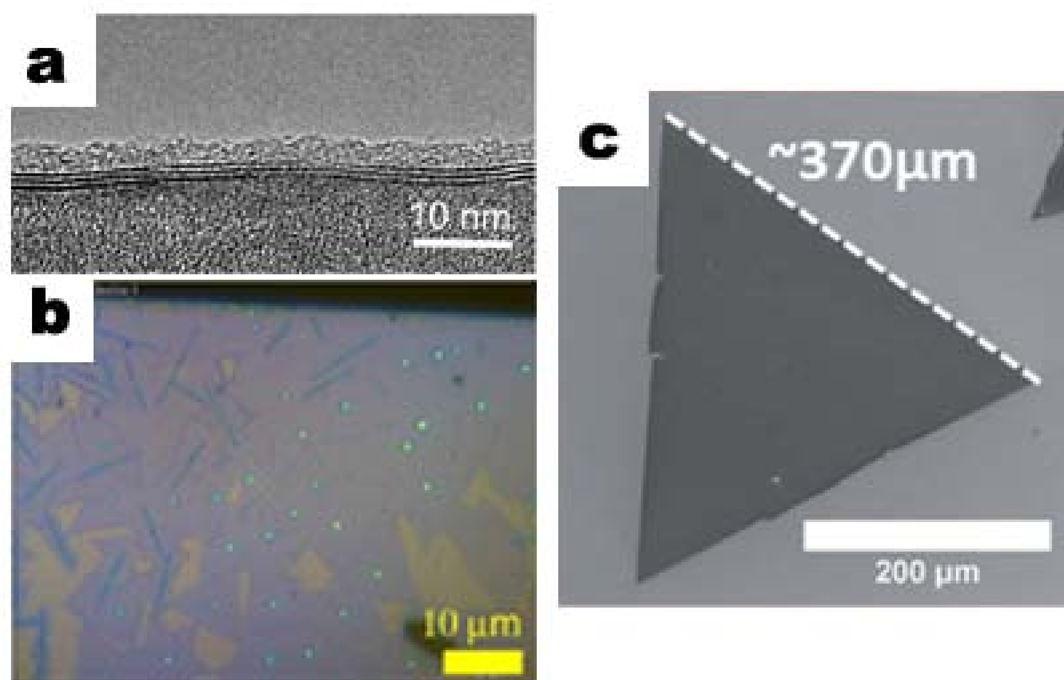

Figure 5. (a) TEM image of CVD grown few layer MoS2, reprinted from ref[73] with permission by John Wiley & Sons; (b) Optical Microscopy image of CVD synthesized single layer MoS2, reprinted from ref[75]with permission by American Chemical Society; (c) SEM image of CVD synthesized single crystal WS_2 nanosheet, reprinted from ref[81] with permission from the Royal Society of Chemistry.

Chemical Science Accepted Manuscript

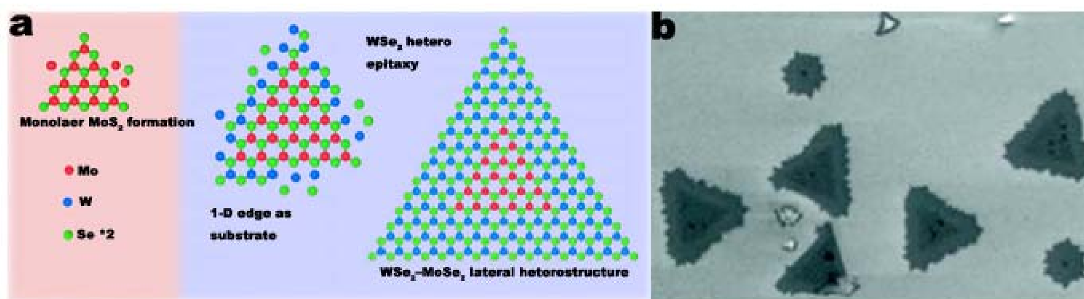

Figure 6. (a) Schematic illustration for the CVD growth process of WSe_2-$MoSe_2$ lateral heterostructure; (b) SEM image of WSe_2-$MoSe_2$ lateral heterostructure. reprinted from ref[85] with permission by American Chemical Society.

Chemical Science Accepted Manuscript

TOC

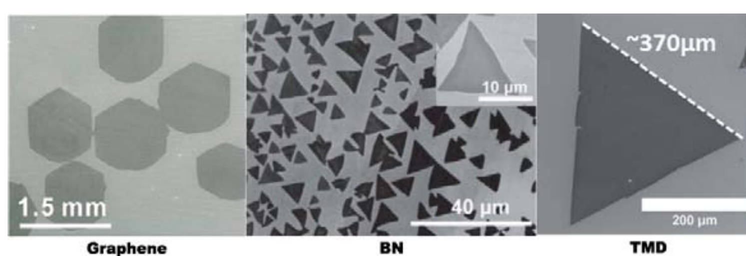

High quality two-dimensional materials such as graphene, BN, transitional metal dichalcogenides by CVD provide new opportunity for large scale applications.

Chemical Science Accepted Manuscript